Creep and Creep-Rupture Properties of the Cladding Tube for Fast Breeder Reactor in High Temperature Sodium. On the 2nd Trial Products for MK-I Core of "JOYO"

Dec., 1975

POWER REACTOR AND NUCLEAR FUEL DEVELOPMENT CORPORATION

T N951 75-10
Dec., 1975

Creep and Creep-Rupture Properties of the Cladding Tube for Fast Breeder Reactor in High Temperature Sodium. On the 2nd Trial Products (AISI Type 316 SS) for MK-I Core of "JOYO"

Shun-ichi Yuhara*
Eiichi Yoshida*
Hideo Atsumo*

Abstract

As the basis for designing the fuel assembly for the sodium cooled fast breeder reactor "JOYO" and for determining the service condition of the reactor core, it has been required to obtain creep and creep-rupture properties of the domestic seamless tubes of AISI Type-316 stainless steel with the nominal dimension of 6.3 mm outside diameter and 0.35 mm wall thickness in flowing sodium environment under various conditions.

For the examination in sodium environment, creep testing apparatuses were designed and incorporated with the two sodium loops for material tests. The sodium handling technique and the testing method up to 700 °C have been established.

The effects of oxygen level in flowing sodium on creep-rupture properties of tubular specimens of Type-316 stainless steel have been examined. At the oxygen levels of 5 and 10 wppm in flowing sodium, the values of creep-rupture strength under uniaxial tension at 600 °,

---

This is the translation of PNC Document N941 75-46 with some improvements.

* Sodium Technology Section, Sodium Engineering Division, Ōarai Engineering Center.

650 °C and 700 °C up to about 2,000 hrs. (the longest rupture time) are not significantly different.

The rupture strength under internal pressure and under uniaxial tension are significantly lower in flowing sodium containing 10 wppm oxygen at 700 °C than in air at the same temperature. Furthermore, the decrease of rupture strength is greater as the exposure time in sodium is longer. And at 700 °C minimum creep rate in sodium is higher than in air. This tendency is remarkable in low stress region.

This apparent reduction in rupture strength is accompanied by the significant decarburization of specimens tested, and the formation of a degraded layer in the neighbourhood of the specimen surface exposed to sodium.

CONTENTS

1. Preface

The thin walled small sized seamless AISI 316 steel tubes, which are designated to be domestically used as the fuel clad tubing for sodium cooled fast breeder reactors in Japan, are irradiated in the following sodium of high temperature in the range of 370 °C to 700 °C, and receive gradually increased internal pressure caused by the fission produced gas generating from the nuclear fuel burn-up inside the cladding tube. Consequently, the creep behavior of fuel cladding tubes under a high temperature sodium environment is an important problem which must be determined and clarified together with their characteristic features under irradiation and in air.

In relation to the creep performance of fuel cladding tubes made of 316 steel and other comparable austenitic stainless steels, there are found hardly any studies made systematically to examine the effect of sodium with sodium purity as parameter, or any comparative studies with in-air data at various different temperatures.

The present research work was aimed to obtain certain basic design data relating to in-sodium creep performance of the domestic made fuel cladding tubes for fast breeder reactors, and also to gain further data as considered necessary under several sodium conditions. That is, together with establishment of the technology for tensile creep test and internal pressure creep rupture test in flowing sodium of high temperature, a series of tests and studies were performed on the trial made cladding tubes of AISI Type-316 steel. In the first place, two kinds of purity conditions of sodium, close to the actual reactor-operating condition, (oxygen concentration of 10 ppm and 5 ppm respectively) were established, and then uniaxial tensile creep test and rupture test under various temperatures were performed, and the resulting data were compared and evaluated

against the in-air data.[1] Then, in the second, an internal pressure creep rupture test was conducted under a single purity sodium environment (oxygen concentration of 10 ppm) to study the correlation between internal pressure and uniaxial tensile creep rupture, and thirdly, the correlation between decarburization and rupture strength was considered.

2. Test Specimens

2-1. Fuel Cladding Tube for Test

The fuel cladding tubes used for the present in-sodium test were seamless tubes made of SUS-316 steel, of which chemical compositions are as shown by Table 1. Those constituent elements as B, N and Co which might pose problems especially in the nuclear reactor core were precisely and minutely specified as to their quantity in the fabrication of tubes. The nominal dimensions of these cladding tubes are 6.3 mm in external diameter and 0.35 mm in wall thickness. The general manufacturing process flow and heat treatment conditions are given as follows:

Steel making (vacuum-melting) → Ingot → Forging → Billeting → Extruding → Rolling → Reduction → Heat treatment (bright annealing 1,000 °C 1,100 °C) → Final cold reduction → Roll-straightening → Smoothing → Final Product Tube

Table 1 Chemical compositions of tested fuel cladding tube for FBR (w/o)

Analysis	Fe	C	Si	Mn	P	S	Cr	Ni	Mo	Co	B	N
Ladle	Bal.	0.07	0.58	1.53	0.003	0.017	16.85	13.18	2.52	0.02	0.0005	0.0276
		0.06		1.52		0.016	16.60	13.14	2.47		0.0004	0.0262
Check	Bal.	0.06	0.57	1.537	0.003	0.013	17.05	13.22	2.41	0.02	0.0002	0.0266
		0.054	0.56	1.51		0.012	16.92	13.14	2.27			0.0258

The cold work rate of the tube billet made by the above process is 10 12 % and the grain size is ASTM No. 7.0 7.1. The test pieces were selected from those which indicated echoes below the standard flow (depth 0.025 mm, length 0.75 mm, V-shaped) by the ultrasonic

flaw detecting method.

The results of the in-air test quoted for the comparison with the results of the in-sodium test were those obtained by employing such cladding tubes which were within the same chemical compositions and the same manufacturing history as those of the in-sodium test.[1)]

2-2. Configuration of Test Specimens

Fig. 1 shows the dimensions and configuration of the test pieces employed for the tensile and internal pressure creep rupture test. Both ends of the tube specimen are welded to the end-plug or the grip-section by TIG welding. For the tensile creep rupture test, tapering or contraction was applied at both end sections of the tube to prevent rupture from the welded section. The gauge length of the test piece was taken between the welded spots of the tapered portion, of which length was about 10-fold of the tube's outer diameter. The test tubes were filled with He gas at the atmospheric pressure (some were filled with Ar gas), while only the exterior surface of the tubes was exposed to or dipped into sodium so that they would be subjected to the identical sodium dipping condition as in the case of the real reactor operation. In respect of the test pieces for the internal pressure creep rupture test, the welded section was reinforced by tightly winding Ni-wire around it to restrain possible deformation of external diameter, thus to prevent rupture from the welded area.

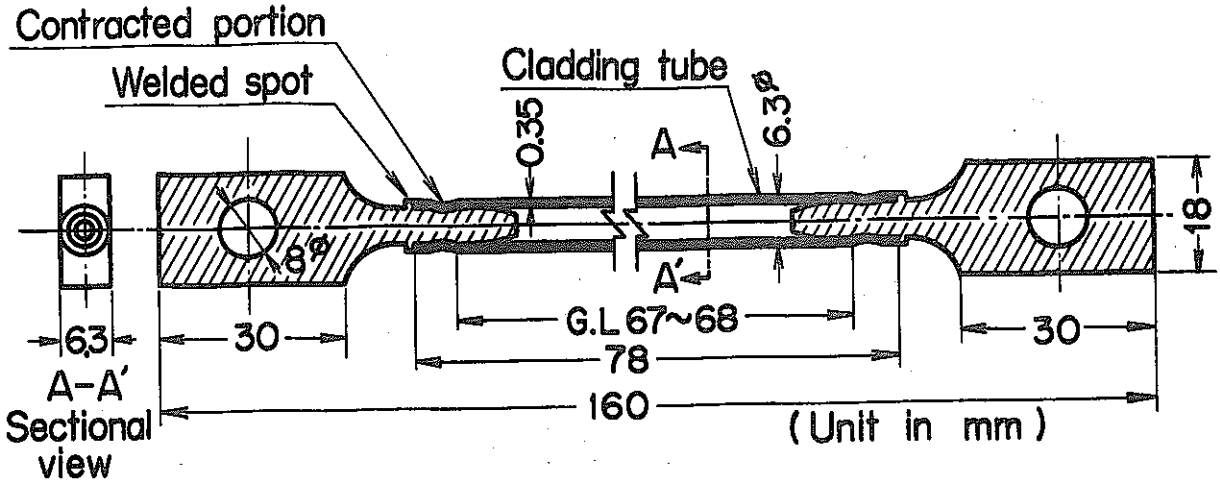

Fig. 1 Shape of specimen for tensile creep-rupture test.

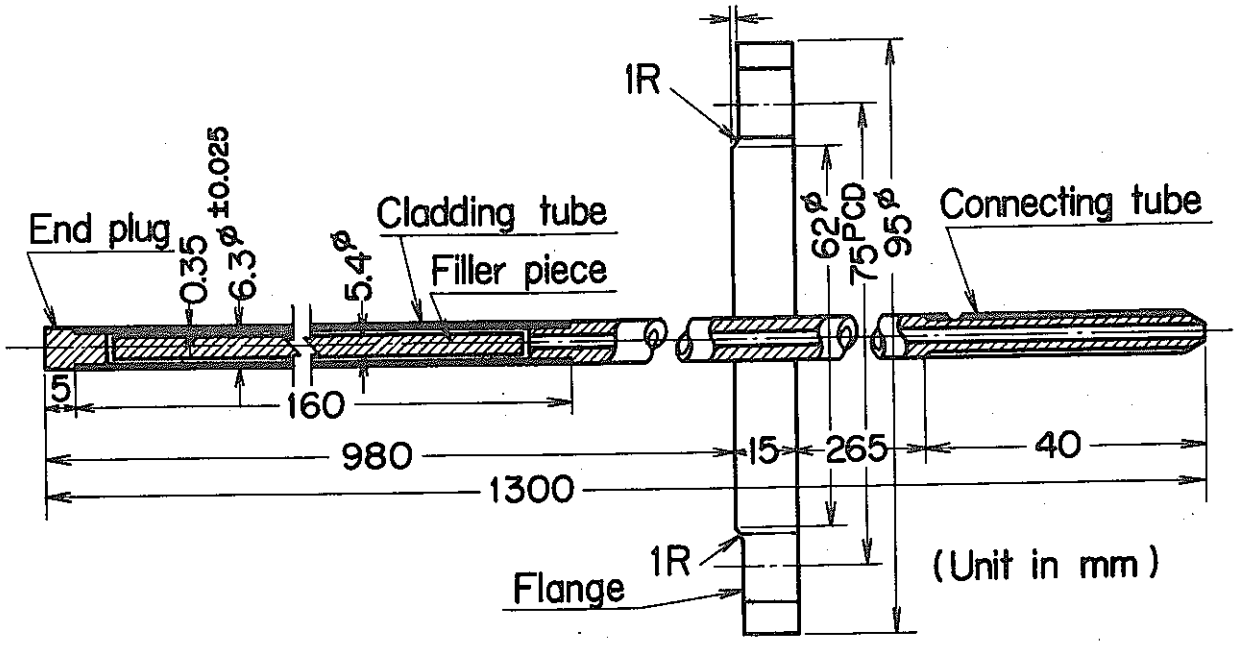

Fig. 2 Shape of specimen for creep-rupture test under internal pressure.

3. Test Loop and Test Method

3-1. Sodium Test Loop

The sodium loops, which were provided for the present experiment are attached to the 2 units of mother loops (a low purity material test loop and a medium purity material test loop). Fig. 3 shows the flowsheet of the internal pressure and uniaxial tensile creep test sections and the mother loop section (the diagram on the right half in thick lines). The mother loop is composed of the purification system with a cold trap and the circulation system with electro-magnetic pumps, and is designed and made to control high temperature sodium purity at

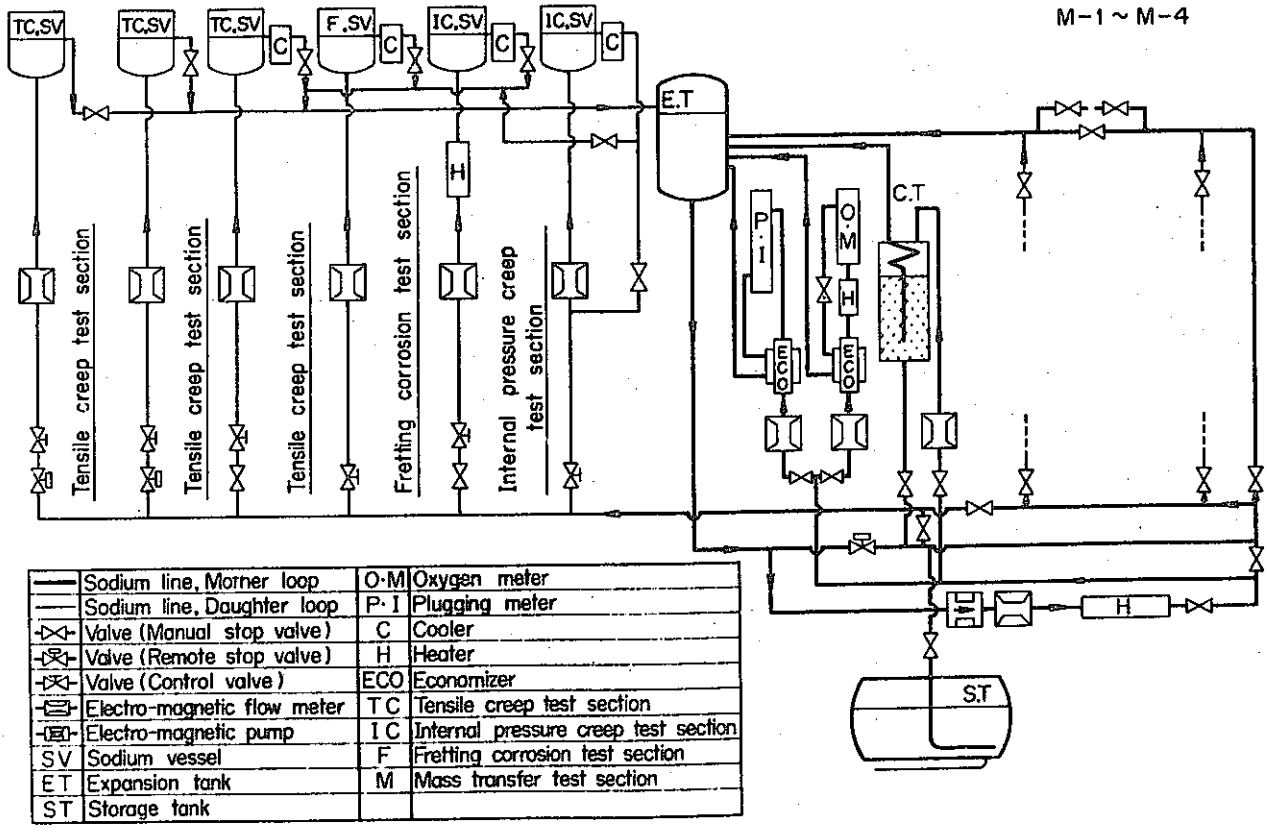

Fig. 3 Flow sheet of the material testing sodium loop.

a constant level. The loops used for the present experiment are made of SUS 316, while the mother loops are of SUS 304.

3-2. Method and Conditions of In-Sodium Test

The tests under the three temperature conditions of 600, 650 and 700 °C were performed in the slowly flowing sodium (flow rate at each test section is about 0.3 litre/min) of certain constant purity supplied from the purified sodium reservoir in the mother loop. The oxygen concentration conditions in the tensile creep rupture test were 10 ppm (chemical analysis mean value by the mercury-amalgam method 9.7 ±1.2 wppm) and 5 ppm (chemical analysis mean value by the mercury-amalgam method 5.5 ±1.1 wppm) respectively. The internal pressure creep rupture test was performed only under the purity condition of 10 ppm. The established temperatures of the cold trap to correspond with these two kinds of oxygen concentration were 190 °C and 145 °C respectively.

The test method was as follows: First, pull-rods fitted with the test pieces of internal pressure creep rupture test or tensile creep rupture test were inserted into the sodium vessel. During this operation flashing of argon gas was continuously applied. Then the sodium vessel and the sodium circulation system were preheated up to 250 °C or 400 °C. Thereafter, sodium of about 300 °C or 400 °C temperature was charged into the vessel from the mother loop. At this temperature level, the sodium was circulated in the loop for about 24 hours for the purpose of preliminary purification. Then, the temperature was raised up to the test temperature. About 20 hours after the temperature arriving at the test temperature, load for each test piece was applied. In the case of the uniaxial tensile creep and creep rupture test, the application of load was made step-wise splitting the weights not more than

about 10 times. For the internal pressure creep rupture test, the internal pressure was applied by the pressured Ar gas. The time required for applying test internal pressure was about 15 min. from the beginning to reaching the test internal pressure. It was possible to maintain the creep test temperature at ±3 °C of the established temperature.

3-3. Creep Tester Installed in Sodium Test Loop

The uniaxial tensile creep tester which is installed in the sodium vessel of the test loop is within the load precision of ±0.5% (within the range of 5% 100% of the load capacity) and of lever ratio of 5 : 1. It is a single unit creep testing machine. The minimum creep rate of the test piece can be given by the creep distortion obtained by the constant measuring of the displacement of the pull-rod. Fig. 4-(a) represents the photograph of the outer appearance of this equipment, and Fig. 4-(b) shows its schematic drawing.

The internal pressure creep test loop is composed of a hydraulic pump, a piston-type pressurizer, a main accumulator a standard pressure indicator, etc. The maximum pressure capacity is 600 Kg/cm^2, and the pressure fluctuation during the loop's operation is absorbed by the accumulator which is controlled at a constant temperature. Fig. 5 represents the schematic diagram of the test loop. The pressure gas employed for the test was Ar gas.

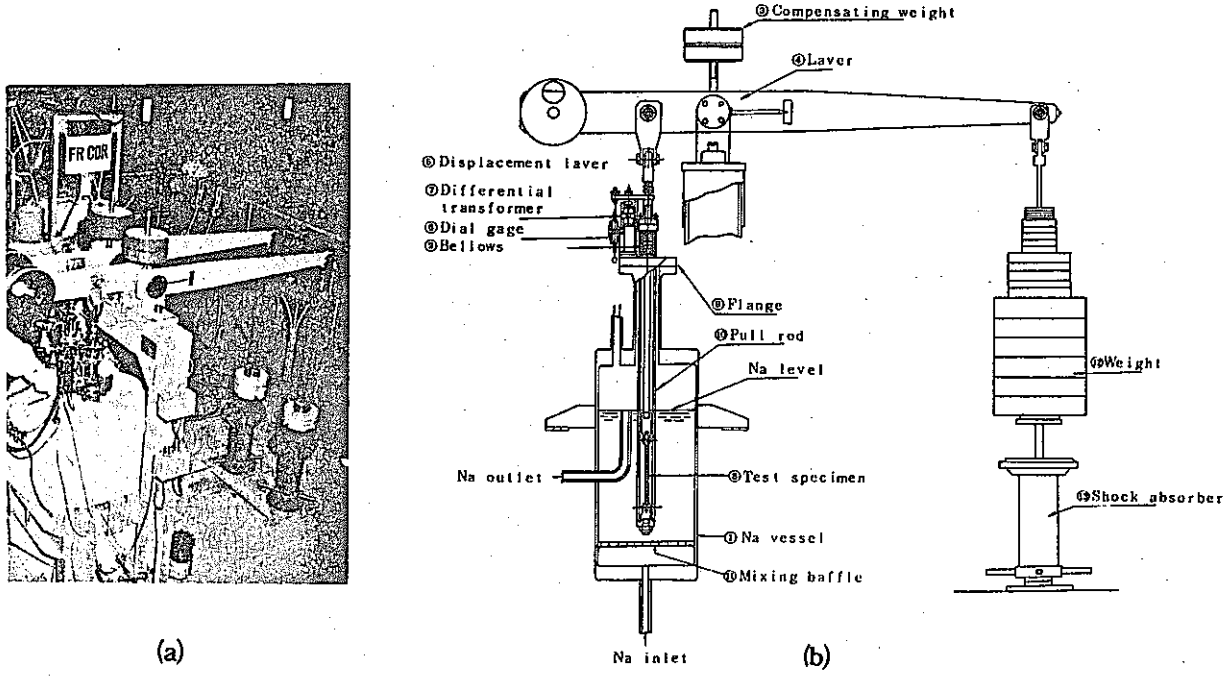

Fig. 4 Tensile creep testing machine affiliated to the material testing sodium loop.

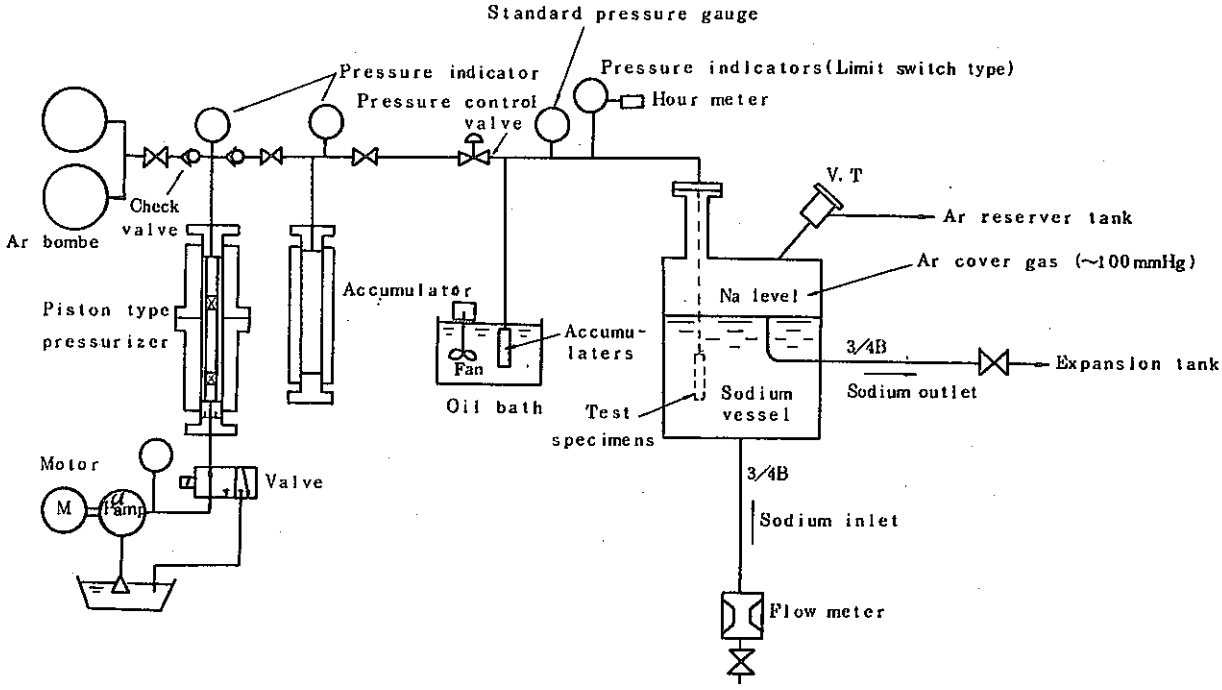

Fig. 5 Schematic diagram of testing apparatus for internal pressure creep test in sodium.

4. Results of Test and Their Evaluation

4-1. Results of Tensile Creep Rupture Test and Internal Pressure Creep Rupture Test, and Their Evaluation

The results of the tensile creep rupture test, which was performed in sodium in which purity condition had been set at 10 ppm and 5 ppm of oxygen concentration, are represented by Fig. 6. As is obvious from the diagram, within the range of the test results obtained up to about 2,000 hours of rupture time, no significant difference was observed of oxygen concentration affecting against creep rupture strength. The general trend of these creep rupture curves is, as shown by the following diagram (Fig. 6), getting lower on the right side toward higher temperature and longer hours. Fig. 7 shows the comparison of data between in-air and in-sodium tensile creep rupture tests. From this, no significant difference between the two at either 600 °C or 650 °C, as longer became the rupture hours, the in-sodium rupture strength

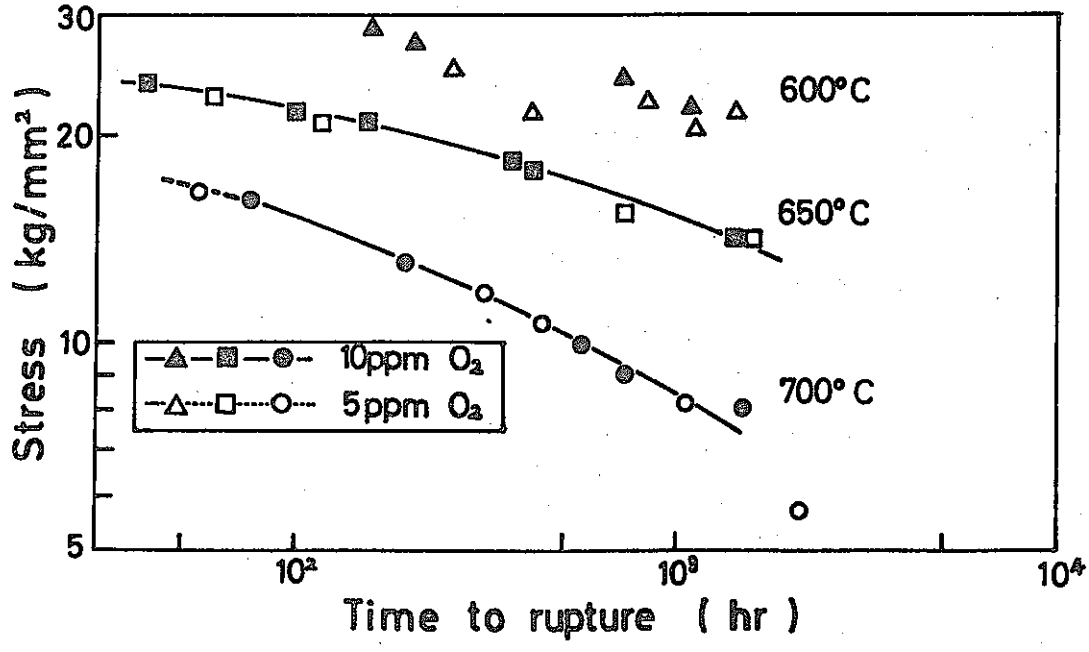

Fig. 6 Comparison of creep-rupture data under uniaxial tension in sodium of 5ppm and 10ppm oxygen.

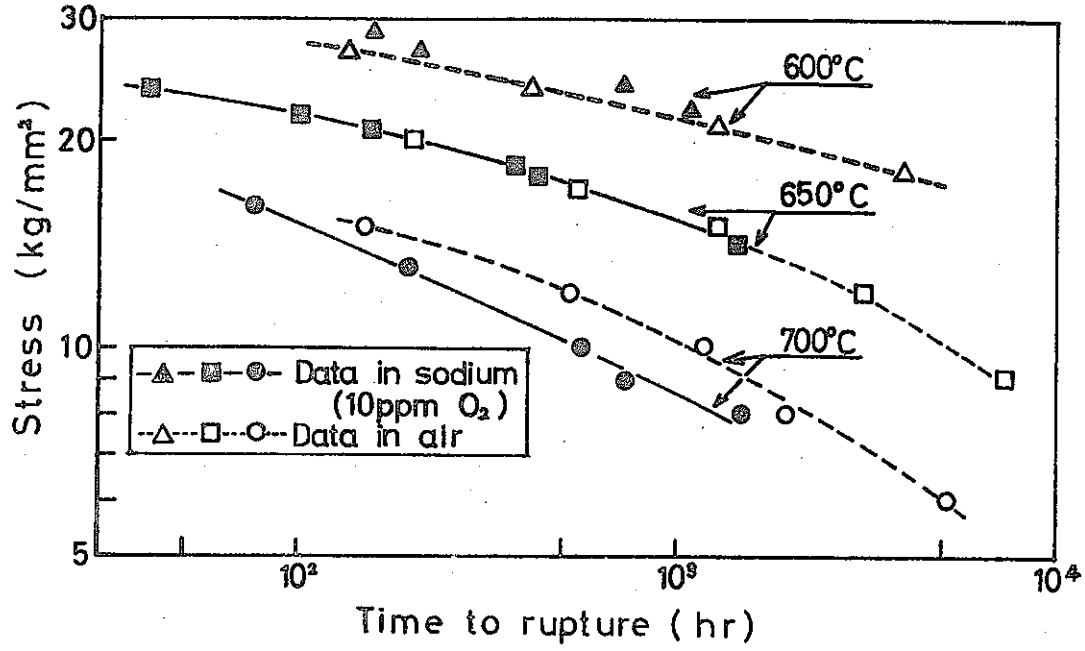

Fig. 7 Comparison of creep-rupture data under uniaxial tension in sodium and air.

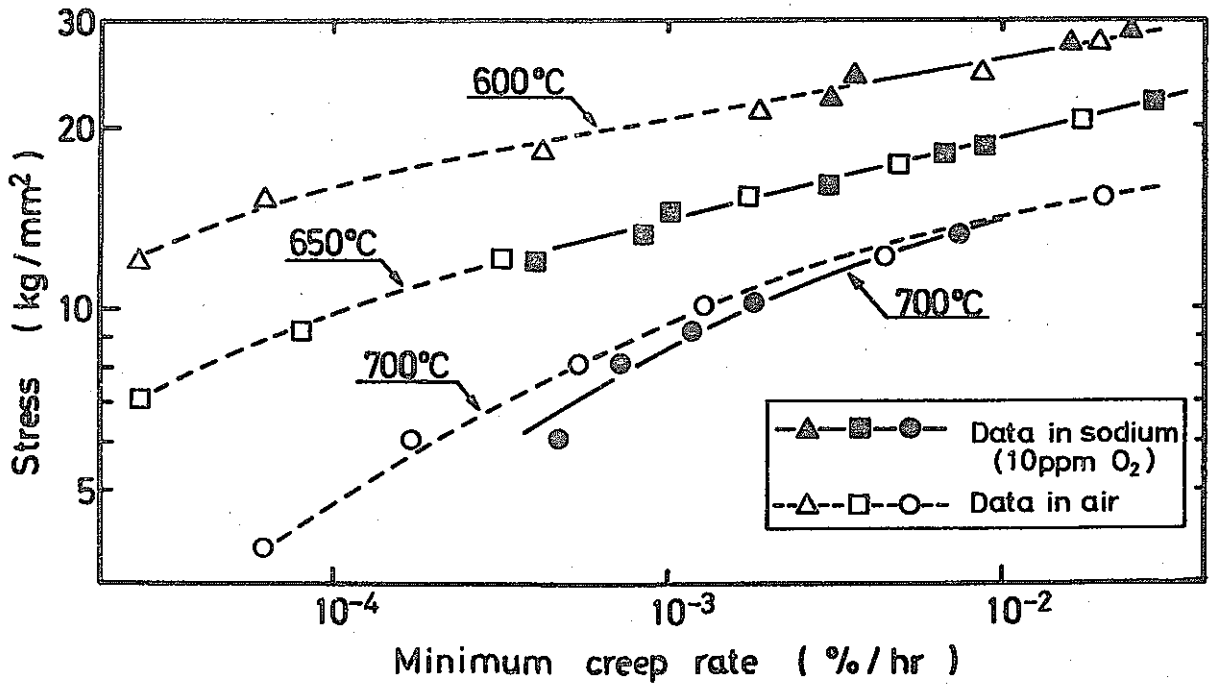

Fig. 8 Comparison of minimum creep rate data under uniaxial tension in sodium and air.

conspicuously declined. Here, the in-sodium creep rupture data were those obtained under the condition of 10 ppm oxygen concentration. The internal pressure of the inert gas packed into the test tube for the in-sodium uniaxial tensile creep rupture test under the atmospheric pressure and at the room temperature will become 2.4 Kg/cm^2 at 700 °C. When this value is converted into the circumferential stress by a mean diameter formula, it is 0.20 Kg/cm^2, and from the fact that this value is not too large as compared with the load stress, its effect is quite negligible.*1 This stress by the internal pressure is alleviated, by the cover gas pressure (about 100 mmHg) in the sodium loop even though very slightly.

The correlation between the minimum creep rate and tensile stress in-sodium and in-air is shown by Fig. 8. Although no significant difference between the two at 600 °C and 650 °C respectively was observed similar to the case of the tensile creep rupture data, the in-sodium minimum creep rate at 700 °C shows a trend of obvious increase on the longer hour side than in the case of the in-air test.

Fig. 9 shows the comparison between the in-sodium data and the in-air data in relation to correlation between the internal pressure and rupture time. The diagram shows that the data of in-sodium internal

---

*1 In order to evaluate the extent of influence of internal pressure, a calculation was made on the most severe case.
At 700 °C (highest temperature in this test range) and 6.0 Kg/mm^2 (minimum value of test stress at 700 °C), sufficiently small values of the ratio $(\sigma^* - \sigma_z)/\sigma_z$ were obtained:

$$\frac{\sigma^* - \sigma_z}{\sigma_z} < 0.5\% \text{ (by Mises' formula)}$$

$$\frac{\sigma^* - \sigma_z}{\sigma_z} < 0.2\% \text{ (by Tresca's formula)}$$

where, σ_z is loaded uniaxial stress and σ^* is Tresca's or Mises' equivalent stress, into which sum of σ_z and stress due to internal pressure is converted.

pressure creep rupture follows the similar trend as in the case of the tensile creep rupture. The decline of in-sodium internal pressure creep rupture strength is about 10 15 % at 1,000 hours (approximately the same rate of decline as in the case of tensile creep rupture strength).

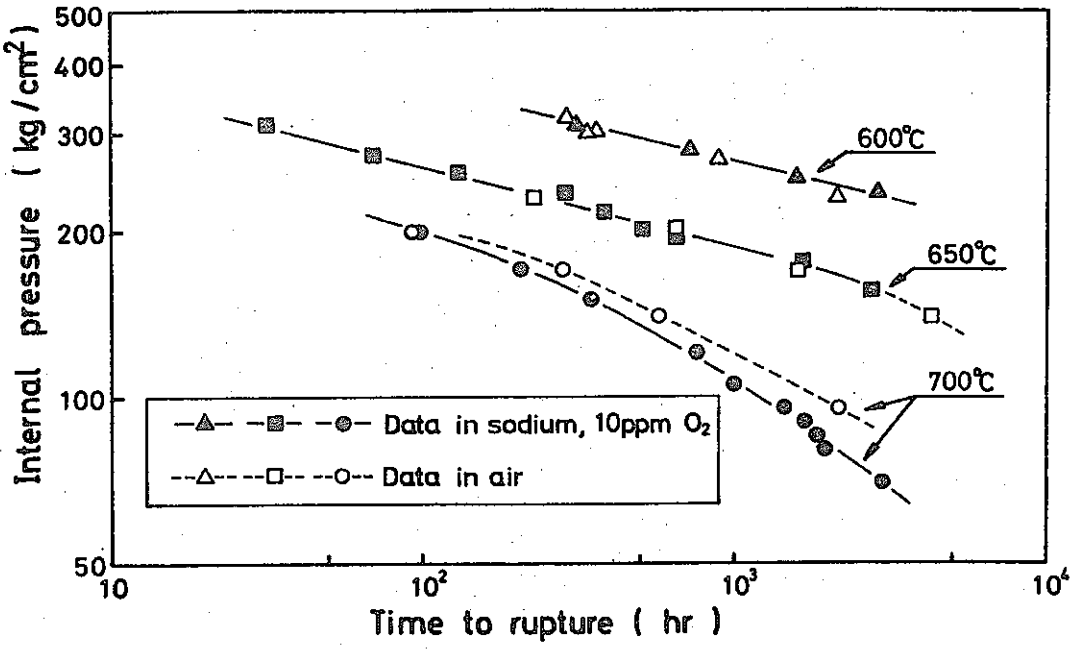

Fig. 9 Comparison of creep-rupture data under internal pressure in sodium and air.

In the next, the internal pressure was substituted by various equivalent stresses, and from the relations between such stress and the rupture time, the correlation between the internal pressure and the tensile creep rupture curves was studied. Following expressions are well known equivalent stress formulas.

Mises' formula: $$\sigma = \frac{3}{2} P \left(\frac{D_o}{2t_K} - 0.5 \right)$$

Inner diameter formula: $$\sigma = P \left(\frac{D_o}{2t_K} - 1 \right)$$

Mean diameter formula: $$\sigma = P \left(\frac{D_o}{2t_K} - 0.5 \right)$$

Outer diameter formula: $\sigma = P\left(\frac{D_o}{2t_K}\right)$

Here, σ : Equivalent stress

p : Test internal pressure

D_o : Outer diameter

t_K : Wall thickness

The resulting data and the tensile creep rupture curves are as shown by Fig. 10. Although there is found no specially matching equivalent stress equation with any tensile creep rupture curve at any test temperatures, those equations which are seemed to match with each other are considered to be the mean diameter equation at 600 °C, the internal diameter equation at 650 °C, and at 700 °C, Mises equation on the relatively shorter rupture time side respectively. If a relatively

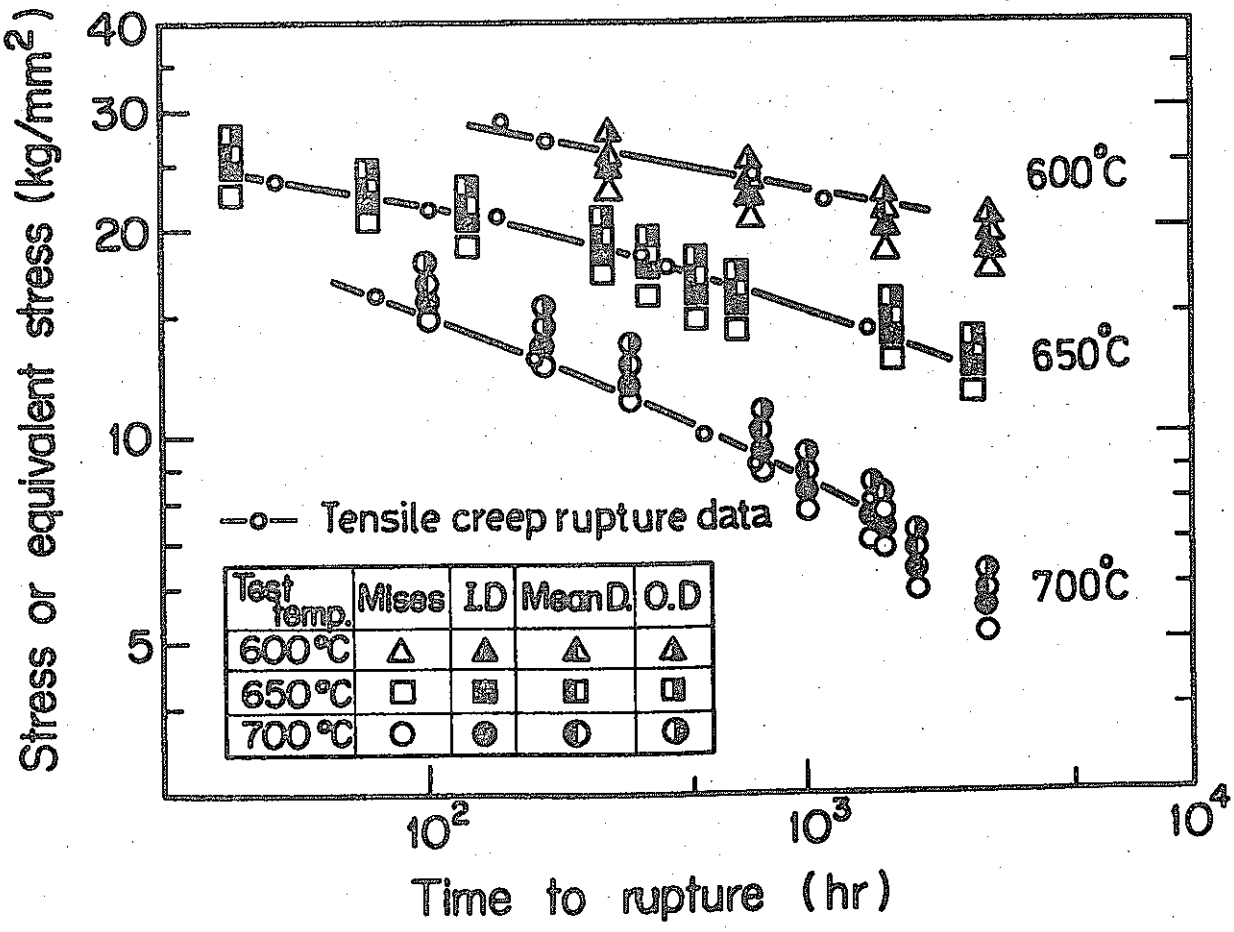

Fig. 10 Comparison of creep-rupture data replaced internal pressure by equivalent stress and tensile creep-rupture data.

well matching equivalent stress equation be selected among these three temperature range, the internal diameter equation might be the one to be cited as well matching. The qualitative trend of these equivalent stress equations which match well with the uniaxial tensile creep rupture curves at each temperature, to give relatively a low stress level, at higher temperature, is very akin to the in-air test data.[2] This is thought to mean that the strength anisotropy was not resulted in by any sodium corrosion effect.

The long hour creep rupture pressure may be obtained from the creep rupture data by applying an extrapolation of a statistical technique using Larson-Miller parameter.[3] Here, studies were made for matching of the curves with a polynomial regression up to the maximum of the fifth order, according to which, the quadratic expression of logarithmic pressure matches best with Larson-Miller parameter under the two environments. Then, by using the mean value of the so obtained parameter constant values of both the sodium and air environment, the matching of the curves was once again worked taking the integral value 14, which was most close to the above mentioned mean value, as the parameter constant, and the following regressive experimental formula was obtained:

Sodium environment: $T(14+\log.t_R)\times 10^{-3} = 3.136 + 15.937 \log P - 4.588(\log P)^2$

In-air: $T(14+\log t_R)\times 10^{-3} = 5.482 + 14.335 \log P - 4.333(\log P)^2$

Here: T : Absolute temperature (^{o}K)

t_R : Rupture time (hr)

P : Pressure (kg/cm^2)

As one example, the rupture pressure at 650 °C at 10,000 hours is obtained as 104 Kg/cm^2 in a sodium environment and 116 Kg/cm^2 in air by extrapolation of the regression curves in each environment. In order to upgrade the accuracy of the estimated value of the creep rupture strength in sodium obtained by a regression expression, it is of course necessary to further study effect of the corrosion in each different temperature. However, the rupture curves as shown in Figs. 7 and 9, indicate the estimated values of the long hour rupture strength at 650 °C to be rather conservative than the actual values.

4-2. Effect of Sodium Environment Upon Creep-Rupture

The external appearance photograph of test pieces after in-sodium internal pressure creep rupture is represented by Figs. 11-(2) and (b) respectively. The cracks associated with the rupture of the test pieces, run along the longitudinal direction of the tube. The ruptured test tubes at 600 °C show cracks, all of which length is one-fold or two-fold as large as the tube's outer diameter. Meanwhile, the ruptured test tubes at 650 and 700 °C show comparatively large crack openings on the shorter rupture time the same as in the case of those at 600 °C. But, as shown by Fig. 11-(b), fine ligamental cracks or pin-hole shaped openings are observed on the long-hour rupture. None of the ruptured test tubes showed any open-door type crack openings. The breaking shape of the in-air ruptured test tubes also presented approximately the similar pattern of openings as in the case of in-sodium ruptured test tubes. However, those of relatively shorter rupture time at 600 °C and 650 °C presented comparatively large open-door shaped openings. These bursting phenomena, when considering the effect on the sodium flow dynamics at the ruptured area and possible release of radioactive

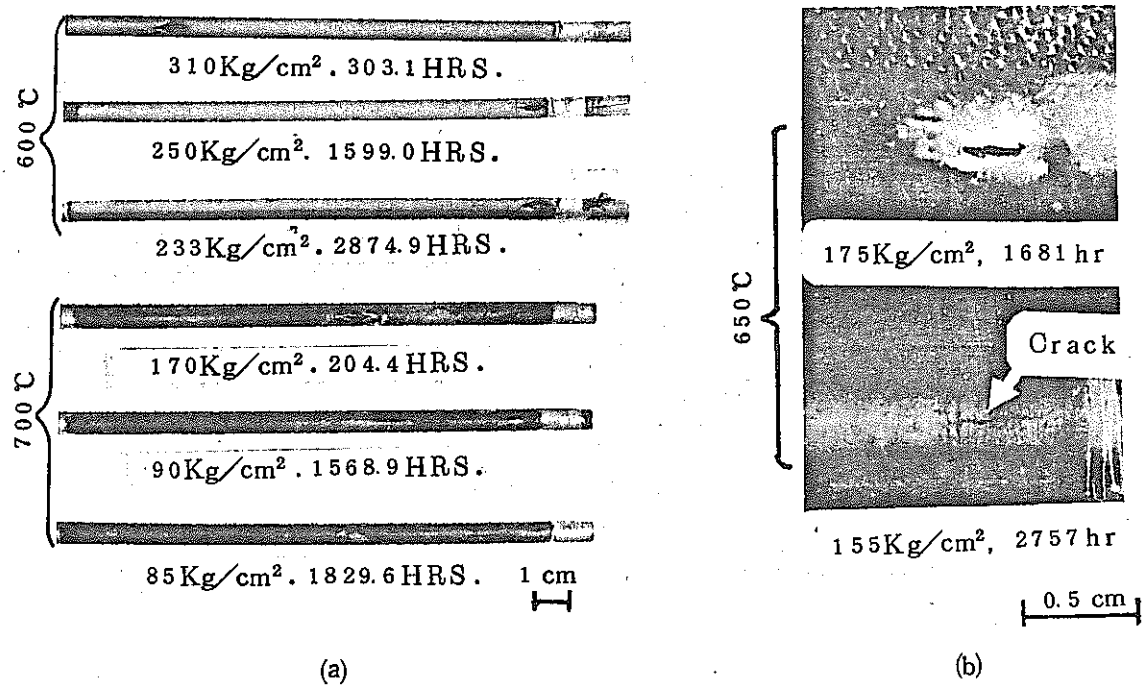

Fig. 11 Appearances of creep-rupture specimens under internal pressure.

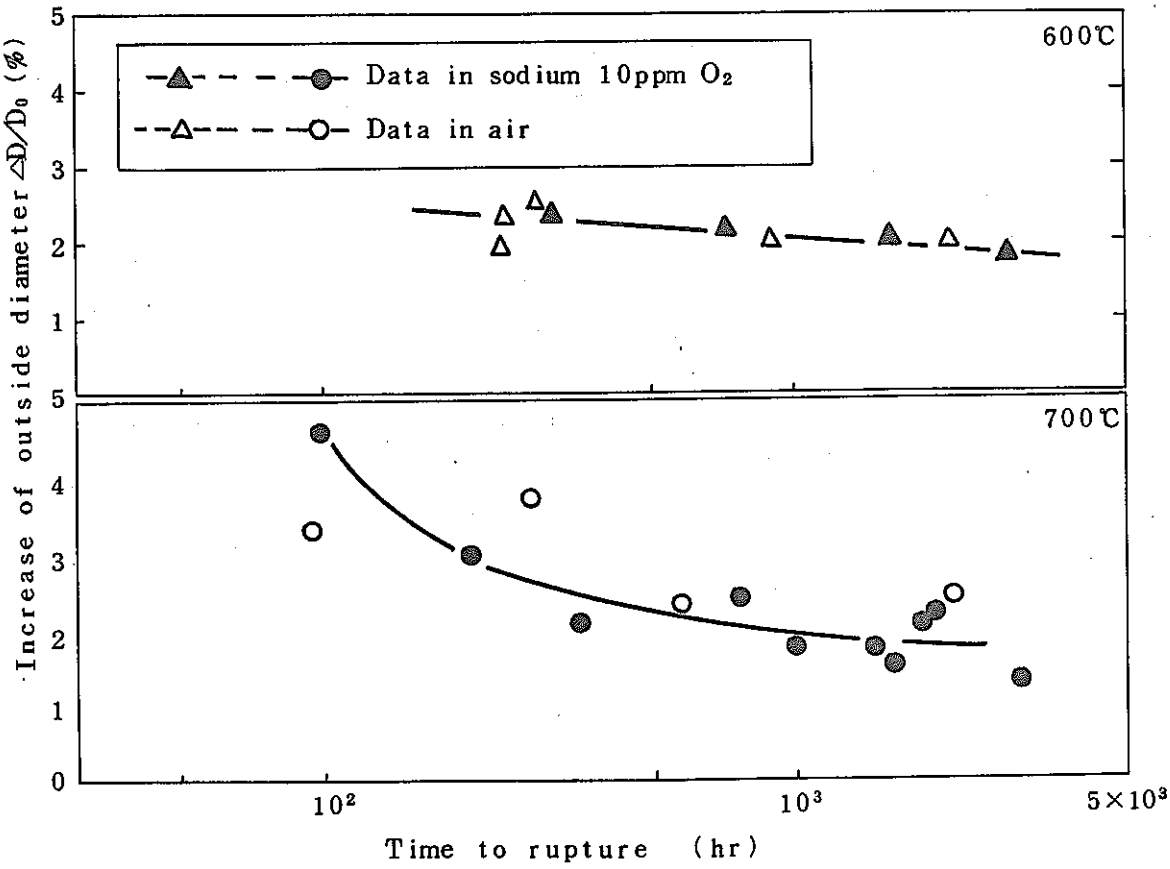

Fig. 12 Increase of outside diameter of specimens ruptured under internal pressure in sodium and in air versus time to rupture.

nuclear fuel and fission gas from these openings, are considered very serious in the actual reactor operation, and are to be taken serious note of together with the irradiated effect of fuel cladding tubes.

The average external diameter increase rates ($\Delta D_o/D_o$) of test tubes after internal pressure rupture at 600 °C and 700 °C both in-sodium and in-air tests, namely the average circumferential rupture expansion, are shown in Fig. 12. Both the in-sodium and in-air tests data at various temperatures show the general trend of decline of average rupture expansion rate down to 1 ∽ 2 % on the longer rupture time or lower stress side. The difference in expansion rates between the tubes of in-sodium test and in-air test at any stages of temperature was not quite clear, and is thought to be within the range of measuring error of both data.

Figs 13-(a) and (b) show the photographs of the sodium dipped surface of the test tubes after in-sodium tensile creep-rupture at 600 °C, and of the tube's longitudinal cross section respectively. This test piece ruptured under the stress of 22.0 Kg/cm^2 at 1,103.4 hours. The sodium exposed surface, as shown by Figs. 13-(a) and 14, presents micro grain boundary cracks in the right angle to the tensile direction all through the area of the gauge length between the tapered end-sections. In the tube's longitudinal cross section, there are observed numerous ligamental cracks, as shown by Fig. 13-(b), on the sodium exposed surface. The pattern of cracks of the in-sodium ruptured test pieces at 650 °C, is observed approximately similar to at 600 °C. From these observations, it is assumed that, at either 600 °C or 650 °C, creep cracks have easily initiated on the sodium dipped surface rather than from the inside where He is filled, and these cracks seemed to progress from the sodium dipped surface into the inner side leading eventually to

tube's rupture. But the creep rupture strength at these temperatures presented no significant difference between the in-sodium and in-air tests. From this, it may be assumed there will be no much difference between in-air and in-sodium tests in the timing for initiation of creep cracks on the sodium dipped surface and the timing for propagation of the major cracks into the tube's interior. But no definite fact has been known.

Fig. 15 shows the sodium exposed surface of the in-sodium creep ruptured test specimens. On the surface of sodium exposed specimens at 600 °C and 650 °C are observed crystalline-formed multi-shaped corrosion products of various sizes with mostly less than 4 μ. At these temperatures, it is assumed that on the sodium exposed surface of the test specimens, dissolution of constituting elements and their deposition are both taken place. As the result of the weighing of the test pieces after exposure to sodium for 1,000 hours, a slight increase of weight

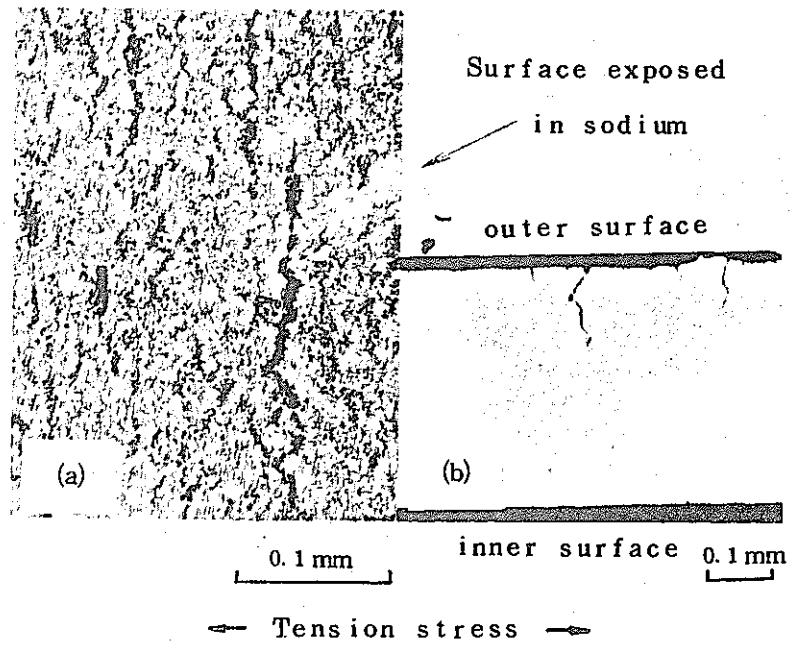

Fig. 13 Crack appearance on the surface of a spcimen exposed in 600°C sodium. (Stress 22.0 kg/mm, Rupture time 1103.4hr)

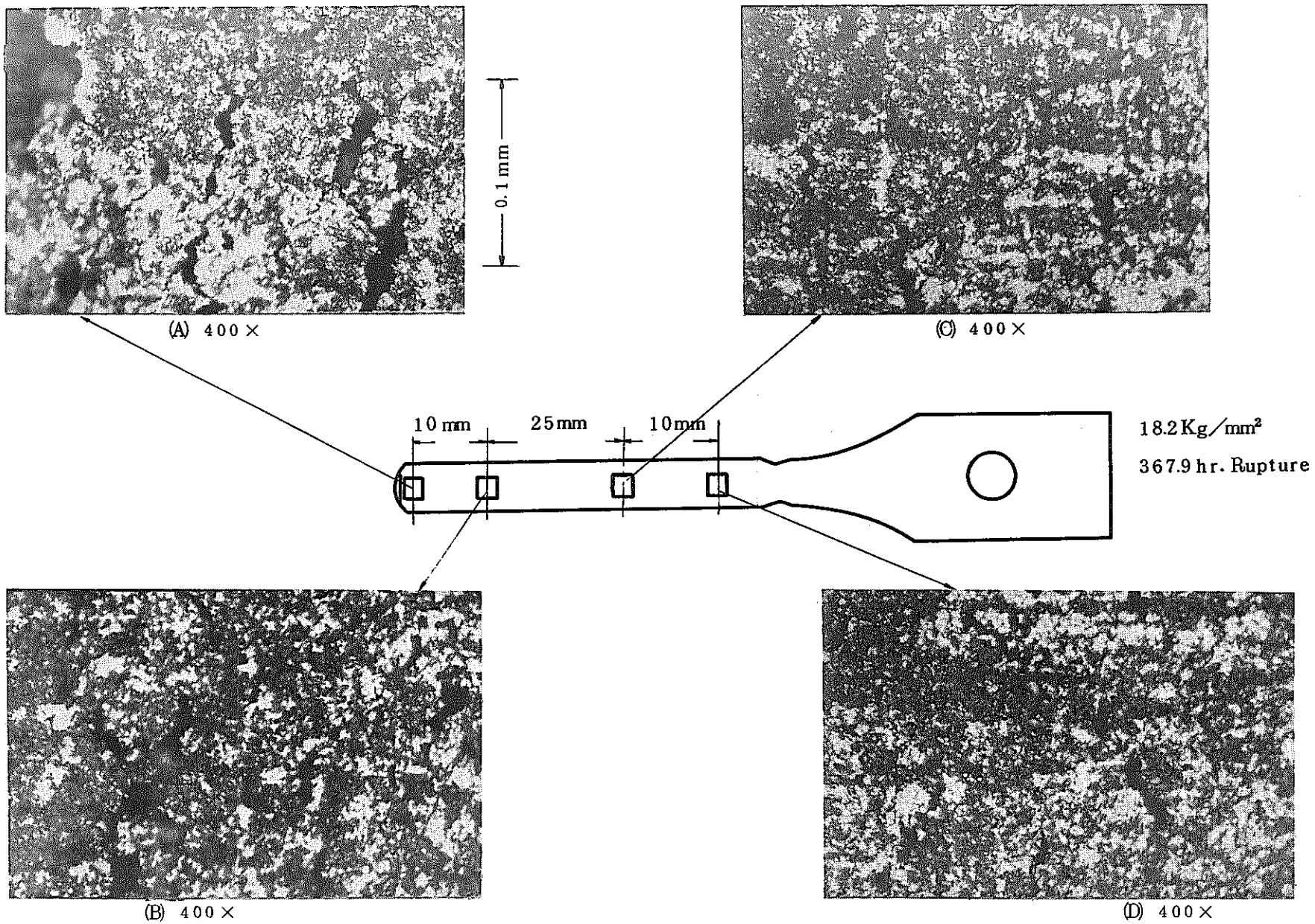

Fig. 14 Surface crack appearances after tension creep-rupture in sodium at 650°C

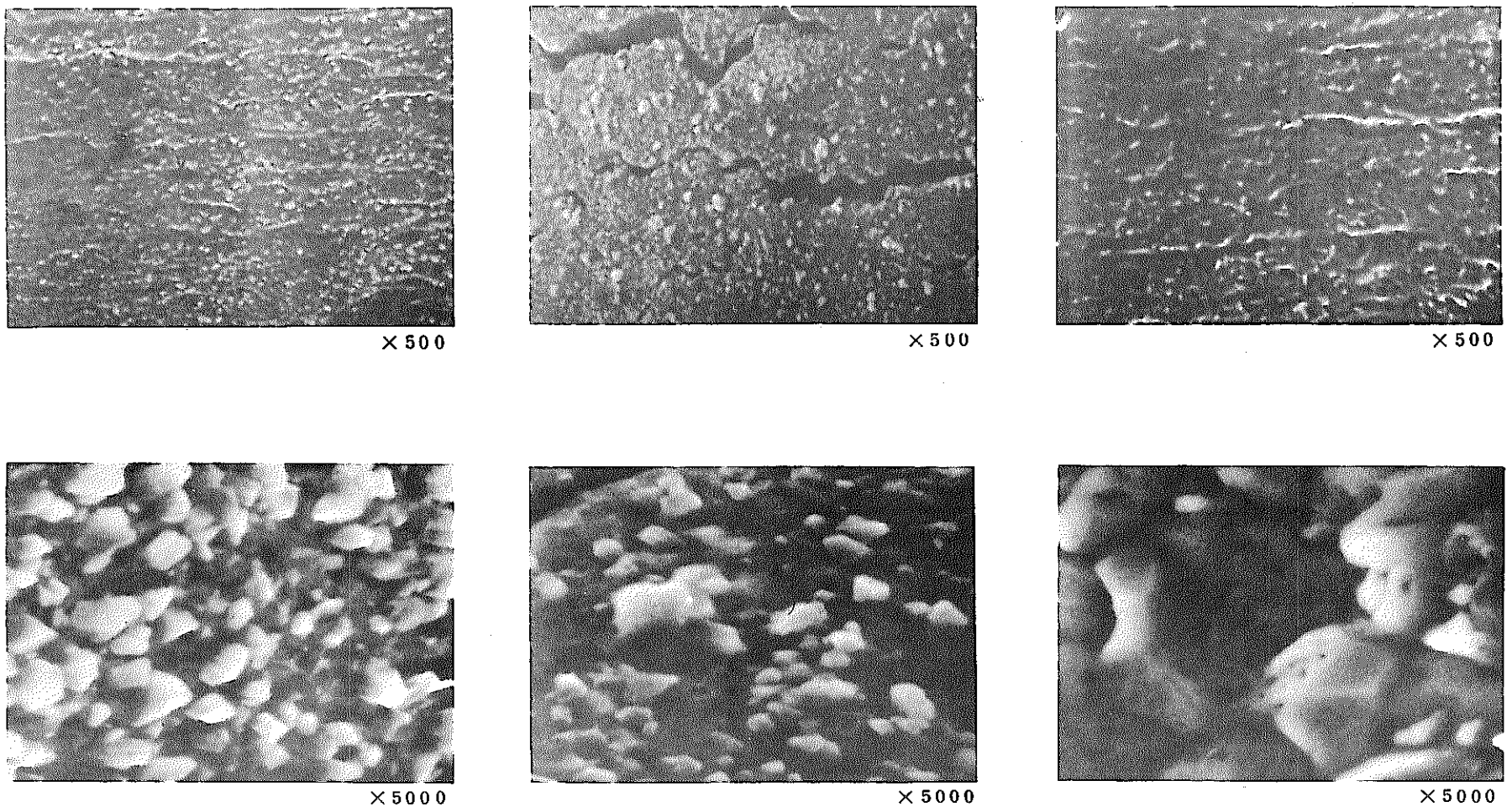

Fig. 15 Scanning electron micragraphs of the surface of the Type 316 cladding tubes exposed to sodium (10 ppm 0) at 600°, 650° and 700°C.

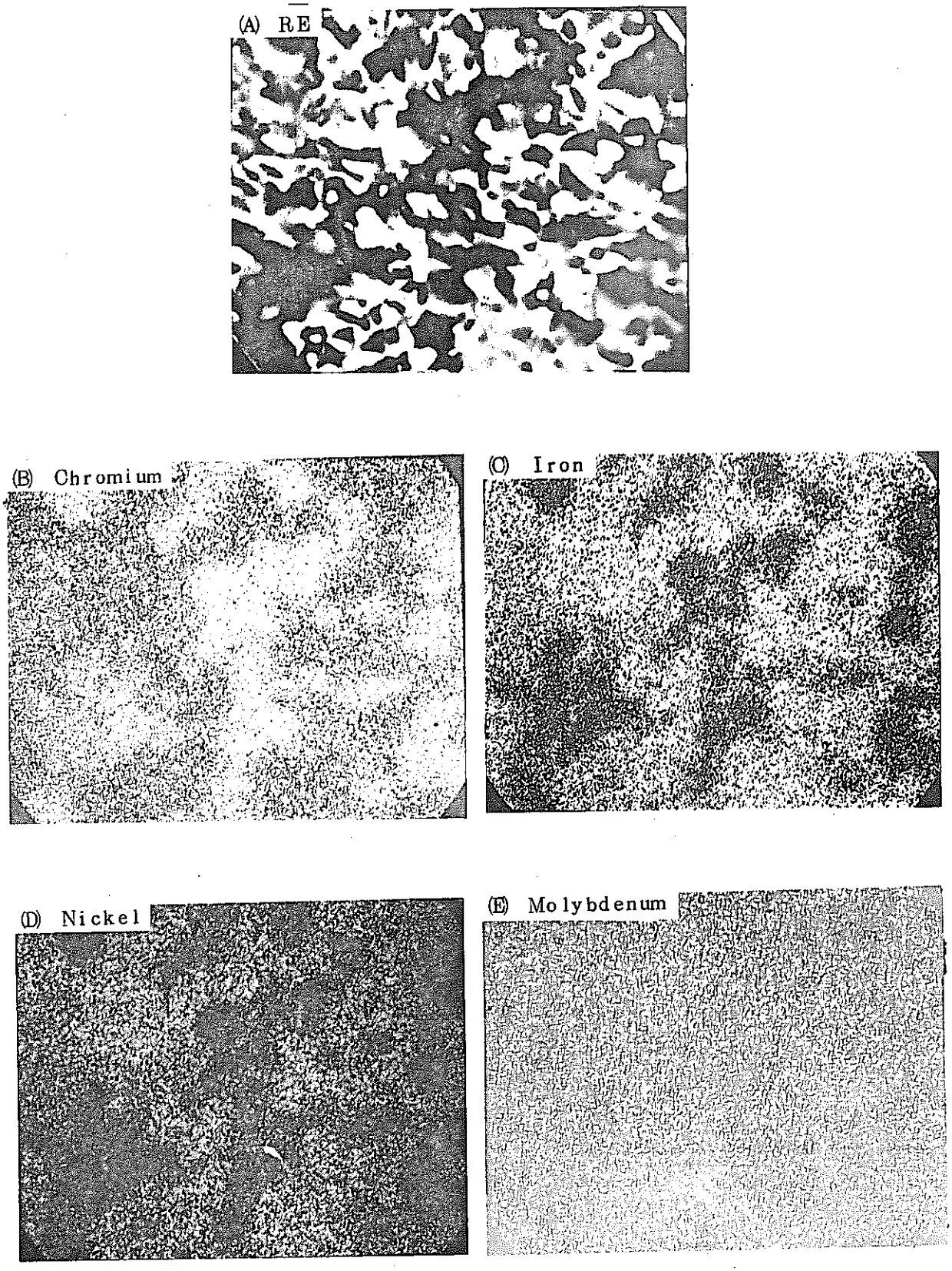

Fig. 16 Xray micrographs of the specimen surface (S3734−10) after exposure in sodium at 650℃ for 800 hours.

was observed comparing with their pre-test weight. This seems to indicate a weight gain because of deposition rather than their weight loss of dissolution. The corrosion products observed on the sodium exposed surface is more possibly thought as the result of deposition rather than degradation of surface. With the test pieces at 700 °C, no much multi-shaped corrosion products were observed. But from the obvious weight decline, the roughened surface and the dented grain boundaries can be assumed to be resulted from the work of dissolution. The cause of such surface roughness may be suggested by the difference in the arrangement directions of each individual grain on the sodium dipped surface, because of which the solution rate of each element differ from each other, and also by comparatively the faster solution rate of elements in the grain boundary regions than other regions of the metal. Fig. 16 represents the corrosion products on the surface of the internal pressure creep test specimens and the X-ray images of the corrosion products deposition and sodium deposition and sodium exposed surface. Fig. 16-(A) shows the reflection electron micrograph (R.E) of multi-shaped corrosion products, while (B) shows the same shape of image with lighter tone than the ground. From these it is concluded that these corrosion products are enriched in chromium. (The shades of X-ray images are in inverse proportion to the quantity of compositions).

The optical microstructures (about 20 mm apart from the ruptured opening) of the test pieces after in-sodium internal pressure creep and creep-rupture tests are shown in Fig. 17. Fig. 17-(a) represents the metallograph indicating the microstructure of the test piece in the case of 600 °C sodium exposure (internal pressure 212 Kg/cm^2, and interrupted after the loading time of 3,015.5 hours). Comparing with the delivered tube billet, there are clearly observed numerous deformation

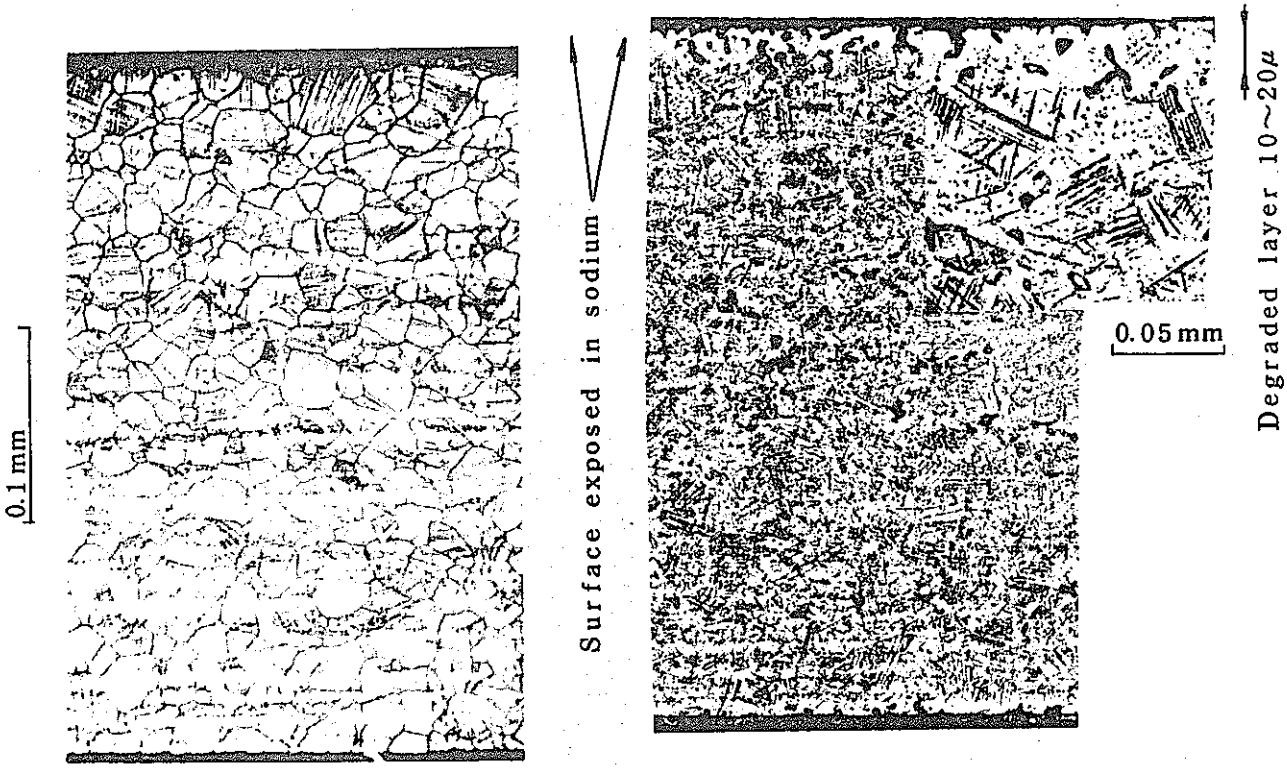

(a) After creep (600°C, 3015.5hr)

(b) After creep-rupture (700°C, 1942.0hr)

Fig. 17 Microstructures after creep and creep rupture tests under internal pressure in sodium.

bands recognizable as parallel lines. At 650 °C, in these deformation bands and grain boundaries, there is observed precipitation of numerous micro particles which are thought to be $M_{23}C_6$.[5] Fig. 17-(b) represents the microstructure in the case of sodium exposure at 700 °C and internal pressure of 80 Kg/cm^2, rupture time 1,942.0 hrs. Inside areas other than the vicnity of the sodium exposed surface, there are noticed increased number of these micro particles appearing all over regardless whether inside or outside of grain boundaries. Also, at the area about 10~20 μ deep inside the sodium exposed surface of the test pieces at 700 °C, there is observed formation of a degenerated layer characteristic to structural change as described below. In this degenerated stratum, unlike the inner structure, hardly observed precipitation of micro particles, and even those deformed ligaments have

almost disappeared. Also is noticed hardness decline, and X-ray diffraction shows no change of grain structure.

Fig. 18 represents the analytical values of carbon content of the test specimens after the tensile creep test and the creep rupture test at each test temperature under the two kinds of sodium purity. The so presented data are the chemical analytical values of fuel cladding tubes of total wall thickness obtained by the combustion method. The numerical figures shown in the diagram represent the sodium exposed

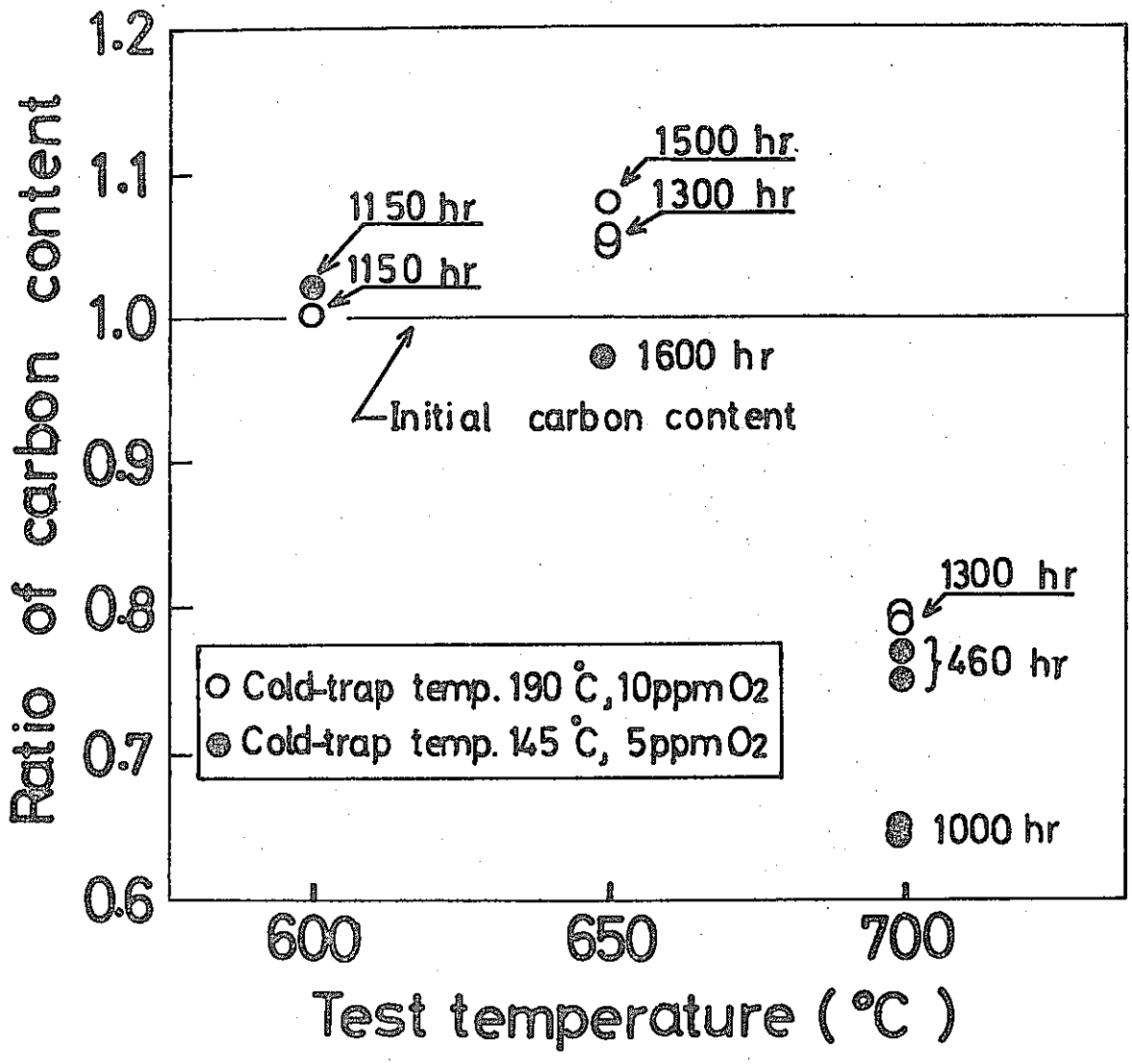

Fig. 18 Changes of bulk carbon contents of specimens after sodium exposure.

time. From this diagram, it is known that decarburization definitely will take place. Where the temperature of the cold trap is 190 °C (oxygen concentration 10 ppm), there is a slight carburization in the sodium at 650 °C, while almost no change is seen at 600 °C. Decarburization is more likely to take place easier at the lower temperature of the cold trap, or on the higher sodium purity side. If it can be assumed that, as the temperature of the cold trap becomes lower the trapping rate of carbon increases, and the in-sodium carbon concentration tends to decline, the results of this experiment are thought to qualitatively agree with the analytical results presented by Snyder who worked on the model of in-sodium decarburization and carburization of austenitic stainless steel.[5] It can be assumed from these results, that considering the effect of decarburization upon material strength, the creep rupture strength at 700 °C on the longer hour side under the condition of the cold trap temperature of 150 °C (oxygen concentration 5 ppm) may sometime decline more than in the case of 190 °C of the cold trap temperature.

Following factors may be considered for the affect of corrosion to the creep performance in high temperature sodium:
(1) General corrosion;*2 (2) Decarburization and carburization; (3) Localized corrosion (for instance, grain boundary); (4) dissolution of micro constituting elements in steel. As to item (1), the annual wall thickness loss in the flowing sodium (flow velocity 3 10 m/sec) with oxygen concentration of 10 ppm at 700 °C is about 25 μ /year.[6] Because of this, the effect brought upon the rupture life

---

*2 Here, the values of weight loss caused by dissolution of constituent elements on the sodium exposed surface of the test pieces are thought to have been converted into wall thickness decline.

upto about 3,000 hours in the slow sodium flow (about 2,000 hrs in the case of the uniaxial tensile creep-rupture test data, and up to about 3,000 hours in the case of the internal pressure creep rupture test data) in the present experiment is thought to be relatively small. As to item (2), there is observed a relative decline of carbon content by about 20～35 % on the sodium exposed test pieces at 700 °C as shown by Fig. 18. From this amount of decarburization and from the relation between the below mentioned carbon content and creep rupture strength, the major factor for the decline of in-sodium creep rupture strength in comparison with the in-air test data at 700 °C is thought to be by decarburization. Correlation has been obtained between the rupture strength at 10,000 hours at 650 °C and carbon of annealed 316 stainless steel, as well as the relation with the quantity of the sum of nitrogen component.[7] According to this, its rupture strength shows decline by about 12 % or 16 % when the steel's carbon content drops from 0.08 w/o to 0.04 w/o. Also when the carbon content of 20 % cold worked material is changed from 0.09 w/o to 0.05 w/o, it has been known that the creep rupture strength at 1,000 hours at 650 °C results in a 16 % decline of strength. With respect to item (3) above, it is suggested from the thickness of its degenerated stratum and the structural change features that the effect upon rupture strength decline at 700 °C is greater than in the case of the effect in item (1), if such a degenerated stratum as indicated by Fig. 12 is included. The effect of dissolution of micro constituent elements in item (4), must be considered in the relation with nitrogen,[7] boron,[8),9] phosphur,[10] etc. But in the present experiment, no investigation on the variation of these microconstituent elements has been undertaken.

As to the extent of the effect which the in-sodium corrosion at 700

^{o}C works upon deterioration of creep performance, the effect of item (2) was the largest within the scope of sodium purity condition, and the next was item (3) which is considered to have been produced in relation with decarburization, and the effect of item (1) is considered comparatively small. The major problems to be clarified in the future studies are effects of micro constituent elements, of sodium flow rate and of sodium exposure time (longer than that of present test) on decarburization and carburization.

5. Conclusion

The following is the summary of the so obtained results:

(1) The creep tester to be installed in the test loop was designed and made to enable the test to be performed maintaining the sodium purity at a constant level. By this, technology for internal pressure and uniaxial tensile creep rupture tests on thin walled, small sized fuel cladding tubes in high temperature sodium up to 700 °C has been established.

(2) The creep rupture strength at the two sodium purity levels (oxygen concentration 10 ppm and 5 ppm) close to the actual operating conditions presents no significant difference within the data obtained by the test up to the rupture time of 2,000 hours. But from the effect of sodium purity on the decarburization, the creep rupture strength in the high purity sodium at 700 °C is thought to be lower on the longer test hours than in the case of low purity sodium.

(3) Comparing the data of in-sodium and in-air tests of both internal pressure and tensile creep rupture, the rupture strength in-sodium at 700 °C in both tests for a long hours creep shows a decline comparing with that of in-air tests. In this relation, the minimum in-sodium creep rate shows the trend of further increase.

(4) Examining the correlation between the in-sodium uniaxial tensile creep rupture and the internal pressure creep rupture, it is known that as the test temperature rises, the equivalent stress equation which shows good correlation with the experimental data moves gradually toward the expression which will give a lower stress level. From the similarity of these transit trends with the in-air test data, it is considered there is no strength anisotropy brought about by the sodium corrosion.

(5) One of the main factors for the relative decline of the in-sodium creep rupture strength at 700 °C in comparison with the in-air test data is considered to be decarburization, and also the degenerated layer on the surface as the result of decarburization is thought to have affected to the deterioration of the creep rupture strength, too.

In this report, the previously reported in-sodium creep rupture test data of the tubes are also employed. The uniaxial tensile creep rupture test data under the oxygen concentration of 5 ppm are based on the referential literature 16) and 17), while those of the internal pressure rupture test are from the referential literature 10), 12), and 15).

At the conclusion of this report, the sincere appreciation of the authors is hereby expressed to all personnel who have made positive contribution to this experimental work, particularly to Mr. R. Saito, Director of Sodium Technology Dept. and Prof. S. Sato of Engineering Institute of Ibaraki University for their great assistance and cooperation.

6. References

1) S. Yoshida, T. Tanaka, I. Ichino and K. Uematsu: International Conf. on Creep and Fatigue in Elevated Temperature Applications, Philadelphia Sessions - September 24-28, (1973).

2) S. Tanaka, S. Yoshida, T. Yachita, R. Nagasaki and S. Yuhara: Journal of the Society of Materials Science, Japan, 20, No. 210, 387 (1971).

3) K. Kawada, S. Yokoi, T. Tanaka, Y. Monma and N. Shinya: Tetsu-to-Hagane (in Japanese), Journal of the Iron and Steel Institute of Japan, 56, 1034 (1970).

4) J.A. Mazza: JISI, 204, 783 (1966).

5) R.B.K. Snyder, Natesan, and T.F. Kassner: ANL-8015, (1973).

6) A.W. Thorley, and C. Tyzack: Alakali Metal Coolant, $SN^{85}/18$, IAEA, Vienna (1967).

7) K. Natesan, T.F. Kassner and Che-Yu Li: Reactor Technology, 15, No. 4, 244 (Winter 1972-1973).

8) M. Fujiwara, H. Uchida, S. Ohta and I. Ishiyama: Tetsu-to-Hagane (in Japanese), Journal of the Iron and Steel Institute of Japan, 60 (1974), S249.

9) T. Yukitoshi and M. Yoshikawa: Research Report of Heat-resisting Metals and Alloys, JSPS123rd Committee, Japan Society for the Promotion of Science.

10) S. Yuhara, T. Furuyama and H. Atsumo: "The Prompt Report (1) of Material Test in Sodium, Internal Pressure Creep and Creep-Rupture Properties of the Nuclear Fuel Cladding Tube for Fast Breeder Reactor", SN943 71-16 (1971).

11) T. Furuya, S. Yuhara, E. Yoshida and H. Atsumo: "Creep and Creep-Rupture Properties of the Nuclear Fuel Cladding Tube (AISI Type 316 SS) for Fast Breeder Reactor in High Temperature Sodium, Internal Pressure Creep Test (I)", SN941 74-11. (1974)

12) K. Nakajima, S. Yuhara, E. Yoshida, T. Owada and H. Atsumo; "ibid., Internal Pressure Creep Test (II)", SN941 73-55 (1973).

13) K. Nakajima, S. Yuhara, E. Yoshida and H. Atsumo: "ibid., Internal Pressure Creep Test (III)", SN941 74-28 (1974).

14) K. Nakajima, S. Yuhara, E. Yoshida, T. Owada and H. Atsumo: "The Prompt Report (3) of Material Test in Sodium, Internal Pressure Creep and Creep-Rupture Properties of the Nuclear Fuel Cladding Tube for Fast Breeder Reactor", SN943 73-03 (1973).

15) K. Nakajima, E. Yoshida, S. Yuhara, T. Owada and H. Atsumo: "ibid., (4)", SN943 74-01 (1974).

16) T. Funada, S. Yuhara, S. Kanazawa, T. Owada and H. Atsumo: "Creep and Creep-Rupture Properties of the Nuclear Fuel Cladding Tube (AISI Type 316 SS) for Fast Breeder Reactor in High Temperature Sodium, Tension Creep and Creep-Rupture Tests under Constant and Incremental Loads (I)", SN941 73-33 (1973).

17) T. Funada, S. Yuhara, T. Owada and H. Atsumo: "ibid., (II)", SN941 74-31 (1974).

Appendix 7.

Uniaxial creep data for the 2nd trial products for MK-I Core of "JOYO"

(Na purity: 10 ppmO)

Temp ℃	No of specimen	Stress (Kg/mm^2)	Time. to Rupture	Minimum creep rate (%/hr)	Exposure time in sodium	Reference
600	S 3737— 1	29. 0	159. 0	2.4×10^{-2}		
	S 3733—22	27. 0	206. 45	1.6×10^{-2}		
	S 3796— 7	24. 0	722. 65	3.55×10^{-3}	～1150	
	S 3758— 4	22. 0	1103. 4	3.12×10^{-3}	～1150	
650	S 3734— 3	26. 4	16. 1	3.5×10^{-1}		
	〃 — 4	23. 7	40. 05	1.2×10^{-1}		
	〃 — 5	21. 7	102. 0	2.8×10^{-2}		
	〃 — 6	20. 9	154. 3	2.5×10^{-2}		
	〃 — 7	18. 2	367. 9	8.9×10^{-3}		
	〃 — 8	17. 6	426. 6	6.9×10^{-3}		
	〃 — 9	15. 7	739. 9	2.1×10^{-3}		Interrupted
	〃 —10	11. 8	739. 9	4.0×10^{-4}	～ 800	
	〃 —16	14. 14	1425. 0	1.06×10^{-3}	～1600	
	〃 —17	12. 99		8.4×10^{-4}	～1600	Interrupted
700	S 3734—18	12. 99	192. 0	7.5×10^{-3}		
	〃 —19	16. 05	75. 4			
	〃 —21	9. 02	725. 8	1.19×10^{-3}		
	S 3758— 1	10. 01	532. 0	1.6×10^{-3}		
	〃 — 2	5. 96	1299. 9	4.7×10^{-4}	～1300	Interrupted
	S 3796— 3	8. 0	1471. 3	7.2×10^{-4}		